Efficient Classification Model of Pneumonia Infection Based on Deep Transfer Learning and Chest X-Ray Images

Muhannad Kassem[*], Baraa M. Albaker[**]

[*,**] *College of Engineering, Al-Iraqia University, Saba'a Abkar Complex, Baghdad, Iraq*

Abstract

Chest X-ray radiographic (CXR) imaging facilitates the early and precise diagnosis of lung disease. Combining CXR imaging with CNN and other artificial intelligence tools can expedite the diagnosis process. Because there are only a small number of clinical images that have been categorized, the most difficult challenge to overcome before these images can be reliably used in disease progression diagnosis is the automated classification of these images as positive or negative cases. A deep-learning approach was proposed to classify lung diseases on CXR images using a transfer learning technique based on the EfficientNetV2 model as the backbone to boost computer-aided diagnosis (CAD) performance reliability and efficiency. The proposed model is trained and tested on the two classifications, normal and pneumonia, based on images from three publicly available chest X-ray datasets. Using the curated dataset of posteroanterior (PA) chest view radiography images, the implemented model achieves an outstanding performance on the tested data represented by an average accuracy of 99.92%. Consequently, it outperforms the most recent classification techniques de-scribed in the literature.

Keywords- Computer-aided diagnosis; Pneumonia, CNN; X-ray, EfficientNetV2B0, Deep learning, Transfer learning.

I. INTRODUCTION

Lung disease, which includes pneumonia, COVID-19, tuberculosis, and other conditions, is one of the primary reasons for people passing away all over the world. For instance, pneumonia is a lung infection that affects the bronchial tubes; some of its symptoms may include coughing, shortness of breath, loss of appetite, fever, vomiting, confusion, low energy, and chest pain with a tingling sensation, which are especially common in the elderly [1]. The diagnosis throughput of human experts, on the other hand, cannot be compared to that of automated systems in terms of difficult to detect early symptoms and may go unnoticed by human beings [2]. Early detection and preserving patients' lives can be significantly improved through evaluation, which can also significantly reduce the life-threatening nature of serious lung diseases. [3]. Imaging technologies, such as CXR and Computerized Tomography (CT), contain extremely potent diagnostic tools that can assist medical professionals in the diagnosis of a wide range of conditions. Currently, a radiologist examines CXR images to detect lung disease. However, these diagnostic tools enable physicians to see inside the body without cutting it. Moreover, x-ray imaging is less expensive, quicker, and more widely accessible than CT, and it exposes the body to significantly less harmful radiation. It is common to use imaging of the chest using CXRs as a diagnostic aid in the screening for pneumonia, and it has been reported to have the excellent prognostic potential [4]. In addition, it is appropriate for use in subsequent examinations due to the increased speed and accuracy with which disease variations could be observed. Despite the complexity of the chest's anatomy, misreading a CXR image is a common source of human error. Consequently, radiologists benefit from the use of CAD Systems in making better clinical decisions and minimizing misreading and timely lung disease detection with high classification accuracy. In contrast to original RGB images, the image obtained from the CXR is one channel of information on grayscale. An X-ray is used to scan the information in the CXR image [5]. X-rays transmit radiation through the body. Calcium-rich tissues, such as bones, are able to block radiation, which results in appearing white on images. The radiation is unable to penetrate soft tissues, such as muscle, liver, heart, and lungs, which results in an image that is gray to the area of black in color. In contrast, the converted grayscale image with three channels contains no new information. As a result, the outcomes from training the Deep Learning (DL) model using learning from the beginning on the data were limited. The quantity and quality, nonetheless of annotated training data are two important factors to consider when developing a detection system. In some research, the DL concept was used to start train from zero on only one grayscale channel, but the outcomes were limited. [6]. To circumvent this limitation, simply collect additional data. The gathering and classification of patient information, on the other hand, requires experts and a significant investment of time and money. Other studies used grayscale images and triplicate the whole process to transform grayscale images of

a single channel into images with three channels [7]–[9]. As being the significant deep learning model for two-dimensional classification, Convolutional Neural Networks (CNN) can better learn and distinguish RGB images than grayscale images. The converted three-channel grayscale image, on the other hand, contains no new information. As a consequence, the CNN trained on the data through the use of learning from scratch produced limited results. Due to the small number of disease samples and the fact that CNN can learn and differentiate to be more specific, on an image with three RGB channels, the application of a transfer learning strategy was the ultimate solution [10]–[12] to transfer the network's weights, parameters, of a model trained on an original three-channel image (source task) and then fine-tune the model on an RGB remade one-channel image (target task). Despite the fact that a CXR image is different from a raw RGB image, the model that was trained on the RGB images may still be able to extract more general features that can assist in the identification of composition, patterns, shapes, and the edges of objects. The classification of lung diseases may also benefit from the use of these characteristics. Using CXR images, this research proposes a DL CNN method that employs the most recent transfer learning technique to distinguish pneumonia lung dis-ease infections. This will assist in enhancing the swiftness and precision of CAD diagnostics. This work focuses on how to improve the performance of pneumonia disease detection using transfer learning with robust hyperparameters based on the most recent EfficientNetV2-b0 CNN architecture.

The remaining sections are arranged in the following fashion: Recent relevant papers are summarized in Section 2. Section 3 explains the methodology used to create, split, and preprocess the dataset. Additionally, the proposed method and training process are introduced in depth. The fourth section presents performance measures, experimental results, and discussions on the proposed methodology. Section 6 outlines concluding remarks.

II. RELATED WORKS

Various fields are already utilizing methods based on deep learning [13]–[16]. Several detection techniques to investigate and evaluate biomedical images, in addition to image categorization, have already been proposed by a variety of authors. M. Razaak [17] discussed the difficulties that lie ahead in computer - aided diagnosis as well as its bright future. According to Dinggang Shen [18], significant progress has been made in the detection of a variety of diseases using techniques based on deep learning. Andre [19] showed how to classify skin cancers at the dermatologist level using a DL method. F. Milletari [20], on the other hand, proposed a CNN-based way to show the prostrate in MRI volumes. Photo-graphs of the retinal fundus can be analyzed using a technique that was proposed by Varun [21] and it can diagnose diabetic retinopathy. Different examination methods [22]–[24] have also been used to come up with ways to use chest X-rays to find diseases. Rajaraman et al. [25], in their study, attempted to explain how customized CNNs work in order to diagnose pneumonia and differentiate between bacterial and viral kinds in the Chest radiographs of children. They used the CNNs to discover pneumonia. Sirazitdinov et al. [26] segmented pulmonary images using a region-based CNN in con-junction with image augmentation in order to detect pneumonia. Rajpurkar et al. [27] utilized deep convolutional neural network with 121 layers, to predict 14 distinct pathologies, one of which was pneumonia, in X-rays that were picked from the frontal view. In [28], fourteen thoracic diseases were DenseNet-121 and feature extraction were used in a localization approach based on prior training to identify. Ayan et al. [29] developed an automatic pneumonia diagnosis system using chest X-ray images. Therefore, an ensemble method consisting of seven pre-trained CNN models was proposed (VGG-16, VGG-19, ResNet-50, Inception-V3, Xception, MobileNet, and SqueezeNet). The dataset comprises 5,856 chest X-ray images representing normal, viral, and bacterial pneumonia. During the evaluation, the final results were obtained by combining the predictions of CNN models with the ensemble method. In chest X-rays, the AUC was 95.21, the sensitivity was 97.76%, and the accuracy was 90.71%, yielding significant results. No image enhancement operations have been made. In addition, accuracy needs further enhancement. Pneumonia was classified by Rahman et al. [30] using deep learning techniques . For the identification of pneumonia, using Mask-RCNN and taking into account both global and local features, Jaiswal et al. [31] successfully segmented pulmonary images. Vikash et al. [32] aggregated the results from several different neural networks using majority voting to arrive at the final prediction. Karthik et al. [33] utilized a custom CNN architecture called shuffled residual CNN. Images of pneumonitis on chest X-rays are collected from many different places and were accurate 99.8% of the time. Hemdan et al. [34] developed the COVIDX-Net model to aid radiologists in identifying and diagnosing COVID-19 in CXR images. They compared the InceptionV3, MobileNetV2, VGG19, DenseNet201, Inception-ResNetV2, ResNetV2, and Xception models, which are all pretrained DL networks. The VGG model had the highest accuracy of 90% based on their tests. B. Antin, J. Kravitz, and E. Martayan [35] suggested a differential classification approach in which X-ray chest images are used as inputs and the outputs are either pneumonia or non-pneumonia in both classes. To detect COVID-19 from CXR images, Sethy P and Behera S [36] Propose a deep learning-based methodology. Eleven pretrained CNN models are used to extract features, and this experiment used the One-Vs-all approach and linear SVM to classify parameters. The performance is evaluated using 25 images for the normal and COVID-19 classes. The model was split into training, validation, and testing using the images' 60%, 20%, and 20% ratios. The best classification accuracy was from ResNet50, with 95.38% accuracy, 97.29% sensitivity, and 93.47% specificity. The few numbers of images (25) for training and testing do not guarantee the system's reliability. Maghdid et al.[37] propose an AI-based tool to aid radiologists in rapidly diagnosing COVID-19 cases from X-ray and CT scan images. The back-bone of the network is a modified, pre-trained AlexNet. This model incorporates 170 CXR and 356 CT images of COVID-19 disease gathered from 5 different sources. During the training phase, datasets are separated into two categories: 50% of the data was used to train CNN, and 50% was used to validate the model three times, In each epoch. The pro-posed CNN models use 50 X-rays and 17 CT images to evaluate performance (not utilized in the training phase). A modified CNN achieves 94.1% accuracy, while a pre-trained network achieves 98.2%. The dataset was split only

for training and testing, with 50% for each set. Rohit et al. [38] proposed the ET-NET framework for a fully automated method for rapid COVID-19 screening that employs a bagging ensemble (bootstrap aggregation) of three transfer learning models (Inception v3, ResNet34, and DenseNet201) to improve the performance of the individual models using chest CT-scan images. The dataset includes 2481 CT-scan images unequally distributed between COVID and Non-COVID categories. 70% (1736 scans) of the images are training data. The remaining 30% (745 scans) for the proposed framework are used as testing data. ET-NET achieved a test accuracy of 97.81%, precision of 97.77%, the sensitivity of 97.81%, and specificity of 97.77%. The dataset is only split into training and testing. Houssein E, Abohashima Z, Elhoseny M, et al. [39] developed a hybrid quantum-classical convolutional neural networks (HQ-CNN) model using random quantum circuits (RQC) to detect COVID-19 and pneumonia patients using CXR images. This study used 5445 images to evaluate the HQ-CNN, including 1350 COVID-19, 1350 normal, 1345 viral pneumonia, and 1400 bacterial pneumonia images. In the initial experiment, the proposed HQ-CNN model achieved 98.6% accuracy and 99.0% recall (COVID-19 and normal cases). In addition, on the third dataset, its accuracy and recall rates were 98% and 98.8%, respectively (COVID-19 and bacterial pneumonia cases). In the multiclass dataset cases, it achieved an accuracy rate of 88.2% and a recall rate of 88.6%. No image enhancement operations have been made.

III. MATERIALS AND METHODS

This section addresses the benchmark datasets for pneumonia diseases in addition to the normal class. Next, the top layers of six pre-trained models is modified to introduce new ones, allowing for more precise classification. The efficiency measurements were finally recorded and plotted on a graph, making it easy to investigate the symptoms and establish what was wrong. Figure 1 shows a normal case and a case with pneumonia disease that were used in this study.

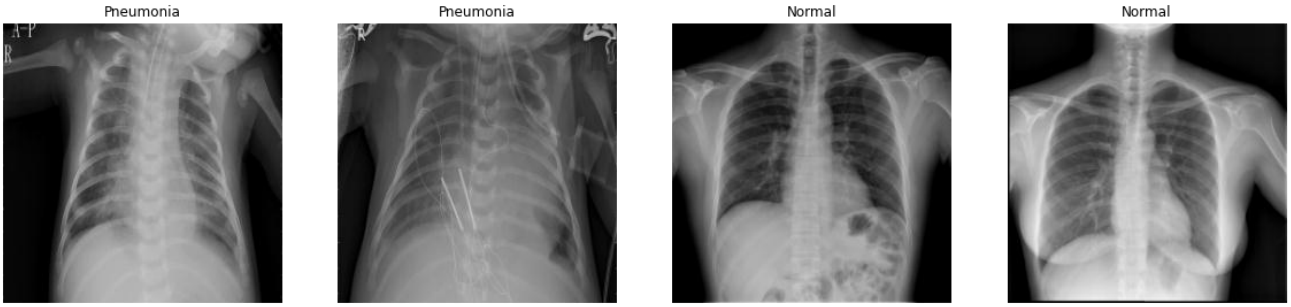

Figure 1. a sample for pneumonia and normal classes.

a. DATASET

i. ORIGINAL DATASET

This study utilized images from three publicly available datasets: PA Chest Radiography Images (X-Rays) v3 [40], NIH [41], and TBX11K [42]. The disease, pneumonia, was selected from the curated dataset and the bacterial and viral pneumonia are combined to form the pneumonia class. Ultimately, the normal class was derived from the NIH and TBX11K datasets. These classes were combined, and we abbreviate the name as the CXR dataset. Figure 2 depicts image distribution information pertinent to the CXR dataset.

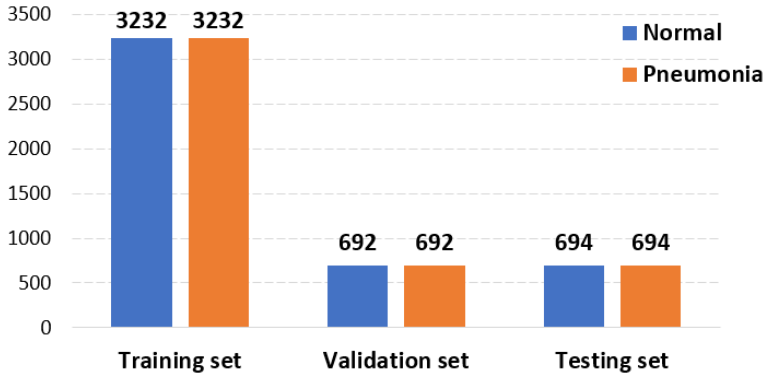

Figure 2. CXR dataset images distribution

ii. DATASET PREPROCESSING

The dataset contains images of varied dimensions and file types. To save time when loading images into the model and to satisfy the model's requirements, area interpolation method are used for downsizing images. The dataset's images were resized to a standard square shape (224×224) prior to loading. The data was then converted to grayscale 3-channel images by deploying it three times (224×224×3). The resultant images are saved in PNG format, and split into three categories: training (70%), validation (15%), and testing (15%).

b. DEPLOYMENT OF EFFICIENTNET

Training efficiency is crucial in classification problems. Therefore, it gains an increased attention by researchers recently by proposing different models and large training data sizes to obtain significantly improved outcomes. However, extending the network's complexity can easily lead to a phenomenon known as "gradient explosion". This phenomenon occurs when significant error gradients build-up while the network is being trained, which causes very large updates to the weights of the neural network model or gradient disappearance, which limits the accuracy improvement. Moreover, storage requirements increase as network depth increases. Also, making the model bigger leads to a lot more information. If the model isn't deep enough, it is challenging to learn complex features. In addition, the model is able to learn more features when the resolution of the input image is increased; however, this results in an increase in the computational cost and a slowdown in the classification process. As a result, as depicted in Figure 3, EfficientNet [38] is a deep CNN that combines the aforementioned three trade-off formats into one to produce the optimal outcome. Figure 3 (a) depicts a baseline network, whereas Figures 3 (b)–(d) depict traditional scaling in which only one dimension of network width, depth, or image resolution is increased. Figure 3 (e) illustrates the central concept of EfficientNet, which is a com-bination of scaling method that enhances the network by scaling all three dimensions uniformly with a constant ratio. Because the CXR dataset was significantly smaller than the ImageNet dataset, transfer learning is adopted to assist in enhancing the generalization ability of our target model. Transfer learning involves the copying of all pre-trained model designs and parameters without header layers. Several of these parameters, like shapes, patterns, edges, and object composition, come from the ImageNet dataset.

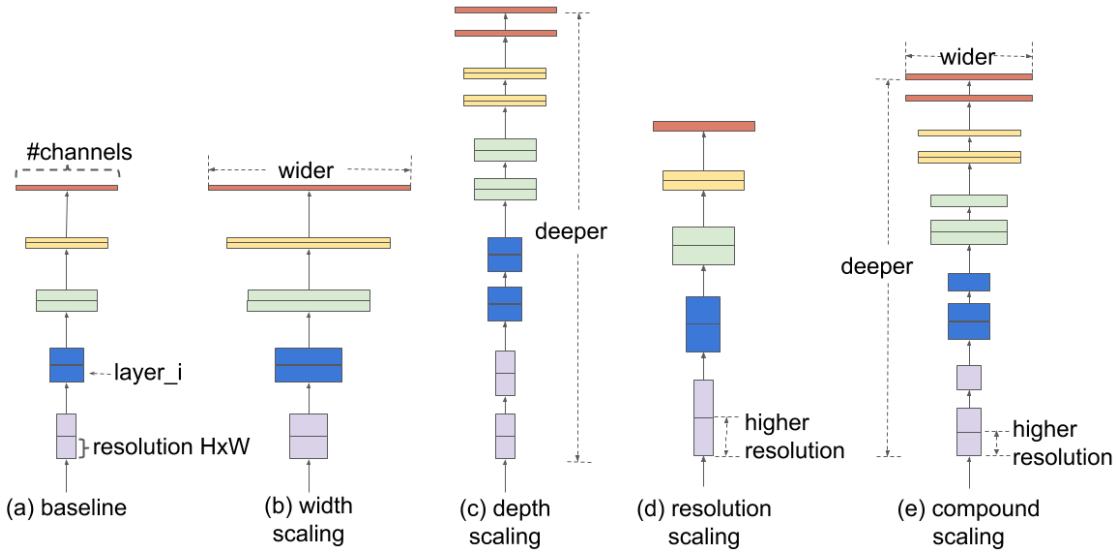

Figure.3 The scaling method in EfficientNet architecture [43]

c. PROPOSED APPROACH

In this paper, a transfer learning technique was implemented using EfficientNetV2 [44] as the backbone architecture. Ef-ficientNetV2 can be trained faster and has better performance than EfficientNet by defining new head layers as a classification model. In order to increase the training speed, enhanced convolution of 1x1 and depth-wise convolution of 3x3 found in MBConv are switched out for the regular 3x3 convolution in the Fused-MBconv segment of EfficentNetV2, that conforms to the key section of the neural network, as demonstrated in Figure 4. Transfer learning typically involves first extracting features from the source dataset (ImageNet) and then transferring them to the global average pooling 2d (GAP2d) layer of the target dataset [45]. Figure 5 provides a visual representation of the proposed transfer learning pipeline.

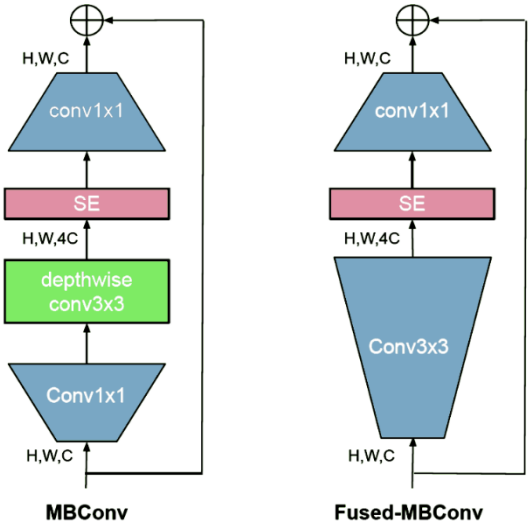

Figure.4 The Architecture of the MBConv and the Fused-MBConv [43], [44]

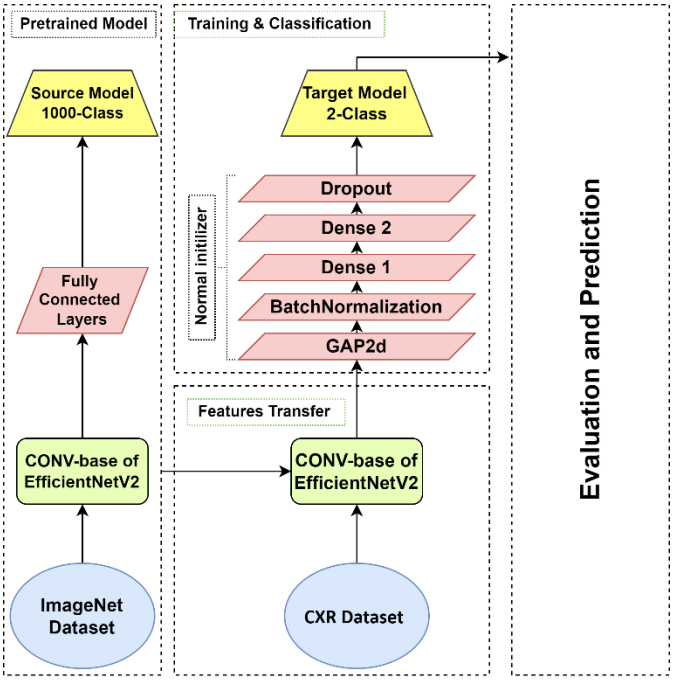

Figure.5. The block diagram of the proposed model.

Before dataset splitting, the normal class was subjected to under-sampling. This is to balance the number of images be-longing to each class. In addition, several call-back functions are deployed including ModelCheckpoint (to save the best weight), EarlyStopping (to stop the training process if the model is overfitting and restore the saved best weights), and ReduceLROnPlateau (to reduce the learning rate when a metric has stopped improving). Due to EfficientNetV2 rapid training speed and efficient parameter utilization, the model and its learned weights were used as our base model during the training phase. The head layers of the proposed models were used to classify the 1000 classes within the ImageNet dataset, as the ImageNet dataset contains 1000 classes. The CXR dataset identified two target classes (normal and pneumonia). In the proposed model, two layers of 2048 units are selected as new head layers and trained using the CXR dataset. The shape of the input layer in the upper part of the layers was 224×224×3. The base model is subsequently frozen to render the conventional base untrainable and the trained weights are maintained. The input tensor is then passed to the model's internal preprocessing input function, which acts as a rescaling layer. The processed data was then fed into the base model. The features then pass from the base model bottleneck to the global average pooling 2D (GAP2d) layer, which is then added to the classification task to aggregate all of the features and overfitting can be reduced by cutting down on the total set of parameters. Then batch-normalization technique was used to dramatically decrease the required number of training epochs for a neural

network, thereby accelerating the learning process and making the net-work more stable during training. Next, all features are then fed into two dense layers (2048 neurons) for training with normal kernel initializer weight and LeakyRELU activation functions. Additionally, a dropout layer is added at a rate of (0.2) to disregard a group of neurons randomly. Typically, this is employed to prevent the net from becoming too tight. In binary classification, the final layer, known as the output dense layer, is composed of one output unit that applies the sigmoid activation function to the features in order to make a prediction regarding the probability of each target class. Table 1 describes in detail the parameters that are produced by the proposed model.

Table 1. The parameters of the proposed target model that was trained on the new head layers of the CXR dataset.

Layer (type)	Output Shape	Parameters Number
Input Layer	(None, 224, 224, 3)	0
EfficientNetV2-b0	(None, 7, 7, 1280)	5,919,312
Global_average_pooling2d	(None, 1280)	0
Batch normalization	(None, 1280)	5120
Dense 1	(None, 1024)	1,311,744
Dense 2	(None, 1024)	1,049,600
Dropout	(None, 1024)	0
Dense 3	(None, 1)	1025
Number of layers in the base model: 270		
Total params: 8,286,801		
Trainable params: 2,364,929		
Non-trainable params: 5,921,872		

The Ranger optimizer is used as a synergistic optimizer that combines LookAhead [46], RAdam (Rectified Adam) [47], and GC (gradient centralization) into one optimizer. Lookahead is a type of stochastic optimizer that updates "fast" and "slow" weights iteratively. The algorithm chooses a search direction by checking the sequence of fast weights produced by a different optimization technique. RAdam is utilized as an inner optimizer to stabilize training at the beginning of training, whereas LookAhead stabilizes training and convergence throughout the remainder of the training. This embed-ding enhanced learning stability by assisting the corrected RAdam optimizer in escaping local minima and decreasing loss variance. In addition, the starting rate (step size) of learning was determined to 0.001, the warmup proportion to 0.1, and the batch size to 32.

IV. Experimentations Results and Discussion

a. The platform for the experiment

The research work is carried out using the GPU run-time type in Google Colab Notebook. Python is used to write the code for the entire approach. The proposed approach includes preprocessing the data and train, validate and test the algorithm to make it suitable to be used for classification. TensorFlow/Keras, Scikit-learn, computer-vision (CV), and NumPy are all adopted and used. The model's hyperparameters are tuned including epochs, loss optimizer, learning rate (LR), and batch size (BS).

b. Results and Discussion

The model was trained with the training set before being validated with the validation set. On the other hand, the model's efficiency and generalizability were validated using the test set, which differs from the training set in that it contains samples that were not included in the training set. As a result, sensitivity (Sen), specificity (Spe), and accuracy (Acc) were selected in order to evaluate the efficacy of the suggested method by utilizing the testing set. This was done so that the effectiveness of the method could be evaluated. Sensitivity is used to figure out how accurate positive predictions are and specificity is used to figure out how accurate negative predictions are, the following equations are used to figure out the right metrics:

$$\text{Acc} = \frac{TP + TN}{\text{TP} + \text{TN} + \text{FP} + \text{FN}} \quad (1)$$

$$\text{Sen} = \frac{TP}{TP + FN} \quad (2)$$

$$\text{Spe} = \frac{TN}{TN + FP} \quad (3)$$

where, TP, FP, TN, and FN stand for true positive, false positive, true negative, and false negative results respectively.

During training and validation, the performance of the proposed model on the CXR dataset was 99.2% for pneumonia and normal CXRs. According to the results, the proposed model performed well in terms of accuracy, sensitivity, and specificity and exhibited no bias or class superiority issues. Figures 6 depict the plots of the performance of the proposed model and the associated confusion matrices. In addition, table 2 provides a summary of the dataset's validation performance.

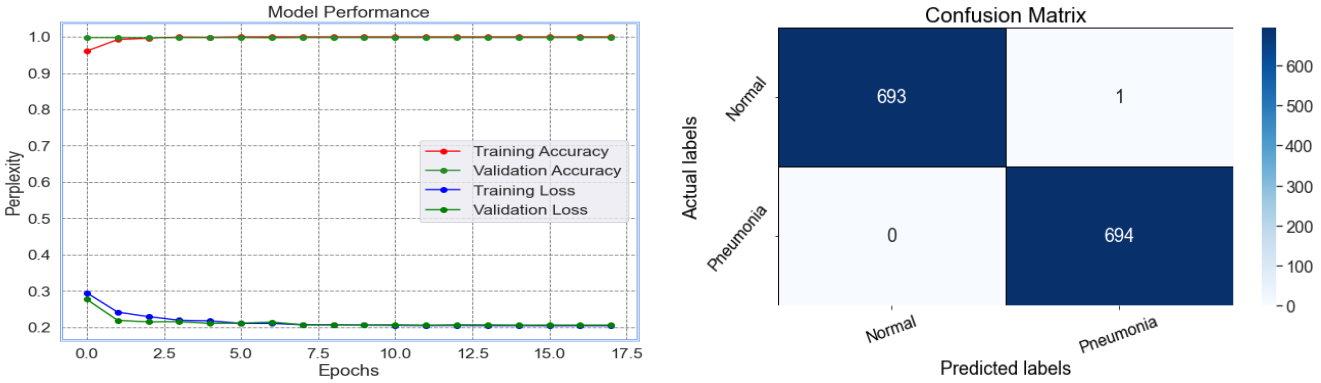

Figure 6. Model performance and confusion matrix for the proposed model when applied to the dataset for two classes (1: Normal, 2: Pneumonia).

As a result, CXRs are diagnosed with the help of the proposed model. The TP indicates that both the true class, normal or pneumonia, of the sample and the result of recognition are positive. Similarly, the FN recognizes a positive real class in the sample, whereas the model labels it as negative. Similarly, FP refers to a negative real sample class that the model recognizes as positive and TN also represents both the true class of the sample and the outcome of the recognition are negative. Both the true-positive rate, also known as the TPR, and the false-positive rate, also known as the FPR, are depicted in the receiver operating characteristics (ROC) of Figure 7.

Table 2. Metrics results for the proposed model using the CXR dataset.

Dataset (experiment)	Class	Acc(%)	Sen (%)	Sep(%)
CXR dataset	Normal	99.92	99.85	100
	Pneumonia	99.92	100	99.92

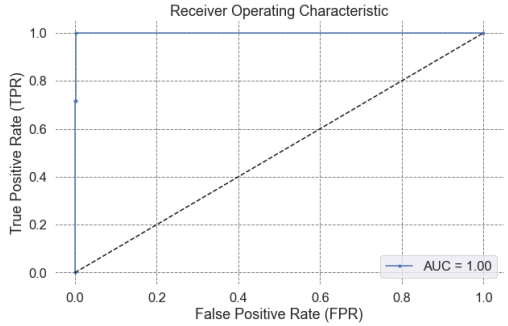

Figure 7. Receiver operating characteristics (ROC) of the CXR dataset.

On the basis of the X-ray image dataset testing set, the predictions for the normal and pneumonia categories are shown in Figure 8. In addition, the predictive probability demonstrates the diagnostic effectiveness of our proposed model for pneumonia. As illustrated in Figure 8, we predicted 12 random images from the test set of the CXR dataset and all tested images were accurately predicted.

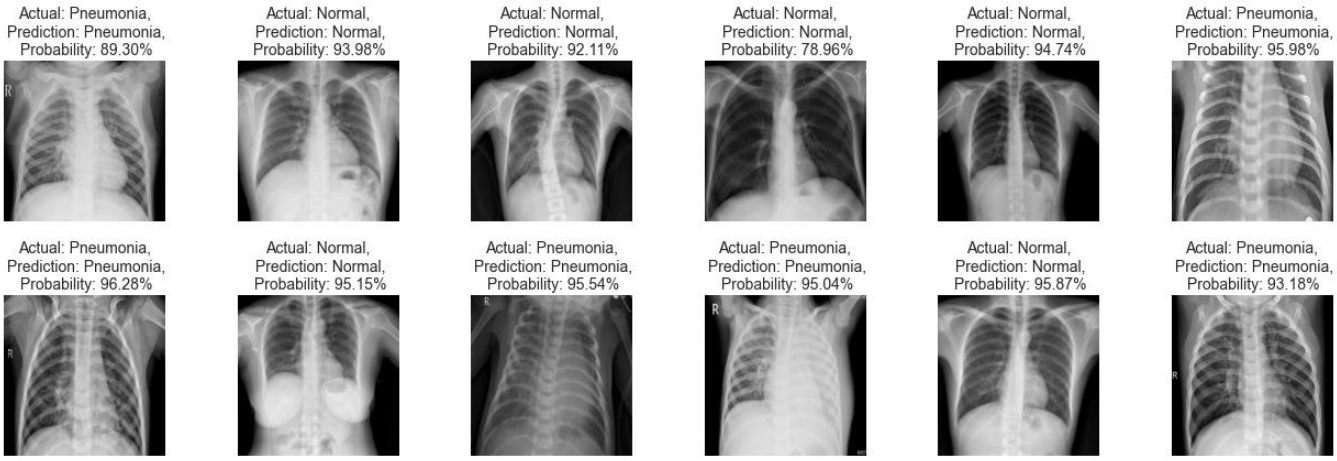

Figure 8. Prediction examples for the normal and pneumonia categories of the testing set of 12 random images of the CXR dataset.

To show the strength of the proposed model for detecting pneumonia from chest X-ray images using binary classification, the model's performance is compared to three state-of-the-art deep learning approaches [34, 36, 37]. Several performance metrics were identified, including model accuracy, time consumption, and complexity. Time consumption is related to the depth of the model, and the complexity is related to the number of parameters produced by the model. Table 3 summarizes the performance comparison among them. The results revealed that the proposed model outperformed them. The proposed model successfully classifies normal and pneumonia with an accuracy of more than 99 %, making it useful for radiologists in diagnosing.

Table 3: Comparison of the results of the proposed model with the other existing state-of-the-art binary methods.

Reference	**Model Type**	**Complexity**	**Training time consumption**	**Accuracy %**
Hemdan et al. [34]	VGG19	143.7 Million	Slow	91
Sethy P and Behera S [36]	ResNet50	25.6 Million	Fast	95.38
Maghdid et al. [37]	AlexNet	61 Million	normal	94.1(modified), 98.2(pretrained)
Proposed model	EfficientNetV2B0	8.2 Million	Very fast	99.92

V. CONCLUSION

Due to the presence of a large number of chest diseases, particularly pneumonia, it is difficult and challenging issue to automatically and efficiently diagnose most potential patients in a timely manner. This is especially true if there is a shortage of physicians or medical equipment. The implementation of techniques involving artificial intelligence can aid in the rapid and accurate diagnosis of diseases via CXRs, and thereby saves a substantial amount of time. In this study, an efficient classification approach for lung diseases based on deep transfer learning of the most advanced CNN model with the Rang loss function was proposed. A classification of the proposed model was developed and trained using the ImageNet pretrained weight of the EfficientNetV2-b0 in order to enhance the diagnostic accuracy of CADs in aspects of their precision and efficiency. Our method achieved an average performance of Sen = 99.92%, Spe = 99.92%, and Acc = 99.92% when predicting the two classes of normal and pneumonia from the CXR dataset. The model's generalization was achieved because there is a negligible performance difference between validation and testing. Therefore, it can be used by medical professionals to automatically diagnose the presence of pneumonia for the patients in a faster and more accurate way.

REFERENCES

[1] S. Levine *et al.*, "The Global Impact of Respiratory Disease THIRD EDITION 2 WRITING COMMITTEE." Accessed: May 30, 2022. [Online]. Available: https://www.firsnet.org/images/publications/FIRS_Master_09202021.pdf

[2] S. H. Wang, V. V. Govindaraj, J. M. Górriz, X. Zhang, and Y. D. Zhang, "Covid-19 classification by FGCNet with deep feature fusion from graph convolutional network and convolutional neural network," *Information Fusion*, vol. 67, pp. 208–229, Mar. 2021, doi: 10.1016/J.INFFUS.2020.10.004.
[3] D. A. Moses, D. Moses MBBS, and F. A. Correspondence Daniel Moses, "Deep learning applied to automatic disease detection using chest X-rays," *Journal of Medical Imaging and Radiation Oncology*, vol. 65, no. 5, pp. 498–517, Aug. 2021, doi: 10.1111/1754-9485.13273.
[4] F. Shi *et al.*, "Review of Artificial Intelligence Techniques in Imaging Data Acquisition, Segmentation, and Diagnosis for COVID-19," *IEEE Reviews in Biomedical Engineering*, vol. 14, pp. 4–15, 2021, doi: 10.1109/RBME.2020.2987975.
[5] "CT Scan Versus MRI Versus X-Ray: What Type of Imaging Do I Need? | Johns Hopkins Medicine." https://www.hopkinsmedicine.org/health/treatment-tests-and-therapies/ct-vs-mri-vs-xray (accessed May 30, 2022).
[6] F. Pasa, V. Golkov, F. Pfeiffer, D. Cremers, and D. Pfeiffer, "Efficient Deep Network Architectures for Fast Chest X-Ray Tuberculosis Screening and Visualization," *Scientific Reports 2019 9:1*, vol. 9, no. 1, pp. 1–9, Apr. 2019, doi: 10.1038/s41598-019-42557-4.
[7] O. Stephen, M. Sain, U. J. Maduh, and D. U. Jeong, "An Efficient Deep Learning Approach to Pneumonia Classification in Healthcare," *Journal of Healthcare Engineering*, vol. 2019, 2019, doi: 10.1155/2019/4180949.
[8] T. W. Kwon *et al.*, "Diagnostic performance of artificial intelligence model for pneumonia from chest radiography," *PLOS ONE*, vol. 16, no. 4, p. e0249399, Apr. 2021, doi: 10.1371/JOURNAL.PONE.0249399.
[9] D. M. Ibrahim, N. M. Elshennawy, and A. M. Sarhan, "Deep-chest: Multi-classification deep learning model for diagnosing COVID-19, pneumonia, and lung cancer chest diseases," *Computers in Biology and Medicine*, vol. 132, p. 104348, May 2021, doi: 10.1016/J.COMPBIOMED.2021.104348.
[10] M. Hong, B. Rim, H. C. Lee, H. U. Jang, J. Oh, and S. Choi, "Multi-Class Classification of Lung Diseases Using CNN Models," *Applied Sciences 2021, Vol. 11, Page 9289*, vol. 11, no. 19, p. 9289, Oct. 2021, doi: 10.3390/APP11199289.
[11] A. T. G. S. FS Yimer, "Multiple Lung Diseases Classification from Chest X- Ray Images using Deep Learning approach," *International Journal of Advanced Trends in Computer Science and Engineering*, vol. 10, no. 5, pp. 2936–2946, Oct. 2021, doi: 10.30534/ijatcse/2021/021052021.
[12] K. el Asnaoui and Y. Chawki, "Using X-ray images and deep learning for automated detection of coronavirus disease," *https://doi.org/10.1080/07391102.2020.1767212*, pp. 1–12, 2020, doi: 10.1080/07391102.2020.1767212.
[13] C. Sun, Y. Yang, C. Wen, K. Xie, and F. Wen, "Voiceprint Identification for Limited Dataset Using the Deep Migration Hybrid Model Based on Transfer Learning," *Sensors 2018, Vol. 18, Page 2399*, vol. 18, no. 7, p. 2399, Jul. 2018, doi: 10.3390/S18072399.
[14] Y. Wang, C. Wang, and H. Zhang, "Ship Classification in High-Resolution SAR Images Using Deep Learning of Small Datasets," *Sensors 2018, Vol. 18, Page 2929*, vol. 18, no. 9, p. 2929, Sep. 2018, doi: 10.3390/S18092929.
[15] Y. Zhang, G. Wang, M. Li, and S. Han, "Automated Classification Analysis of Geological Structures Based on Images Data and Deep Learning Model," *Applied Sciences 2018, Vol. 8, Page 2493*, vol. 8, no. 12, p. 2493, Dec. 2018, doi: 10.3390/APP8122493.
[16] C. Douarre, R. Schielein, C. Frindel, S. Gerth, and D. Rousseau, "Transfer Learning from Synthetic Data Applied to Soil–Root Segmentation in X-Ray Tomography Images," *Journal of Imaging 2018, Vol. 4, Page 65*, vol. 4, no. 5, p. 65, May 2018, doi: 10.3390/JIMAGING4050065.
[17] M. I. Razzak, S. Naz, and A. Zaib, "Deep Learning for Medical Image Processing: Overview, Challenges and the Future BT - Classification in BioApps: Automation of Decision Making," *Springer*, vol. 26, pp. 323–350, 2018, Accessed: Jun. 19, 2022. [Online]. Available: https://doi.org/10.1007/978-3-319-65981-7_12
[18] D. Shen, G. Wu, and H. il Suk, "Deep Learning in Medical Image Analysis," *https://doi.org/10.1146/annurev-bioeng-071516-044442*, vol. 19, pp. 221–248, Jun. 2017, doi: 10.1146/ANNUREV-BIOENG-071516-044442.
[19] A. Esteva *et al.*, "Dermatologist-level classification of skin cancer with deep neural networks," *Nature 2017 542:7639*, vol. 542, no. 7639, pp. 115–118, Jan. 2017, doi: 10.1038/nature21056.
[20] F. Milletari, N. Navab, and S. A. Ahmadi, "V-Net: Fully convolutional neural networks for volumetric medical image segmentation," *Proceedings - 2016 4th International Conference on 3D Vision, 3DV 2016*, pp. 565–571, Dec. 2016, doi: 10.1109/3DV.2016.79.
[21] V. Gulshan *et al.*, "Development and Validation of a Deep Learning Algorithm for Detection of Diabetic Retinopathy in Retinal Fundus Photographs," *JAMA*, vol. 316, no. 22, pp. 2402–2410, Dec. 2016, doi: 10.1001/JAMA.2016.17216.
[22] U. Avni, H. Greenspan, E. Konen, M. Sharon, and J. Goldberger, "X-ray categorization and retrieval on the organ and pathology level, using patch-based visual words," *IEEE Transactions on Medical Imaging*, vol. 30, no. 3, pp. 733–746, Mar. 2011, doi: 10.1109/TMI.2010.2095026.
[23] S. Jaeger *et al.*, "Automatic tuberculosis screening using chest radiographs," *IEEE Transactions on Medical Imaging*, vol. 33, no. 2, pp. 233–245, Feb. 2014, doi: 10.1109/TMI.2013.2284099.
[24] J. Melendez *et al.*, "A novel multiple-instance learning-based approach to computer-aided detection of tuberculosis on chest X-rays," *IEEE Transactions on Medical Imaging*, vol. 34, no. 1, pp. 179–192, Jan. 2015, doi: 10.1109/TMI.2014.2350539.
[25] S. Rajaraman, S. Candemir, I. Kim, G. Thoma, and S. Antani, "Visualization and Interpretation of Convolutional Neural Network Predictions in Detecting Pneumonia in Pediatric Chest Radiographs," *Applied Sciences 2018, Vol. 8, Page 1715*, vol. 8, no. 10, p. 1715, Sep. 2018, doi: 10.3390/APP8101715.

[26] I. Sirazitdinov, M. Kholiavchenko, T. Mustafaev, Y. Yixuan, R. Kuleev, and B. Ibragimov, "Deep neural network ensemble for pneumonia localization from a large-scale chest x-ray database," *Computers & Electrical Engineering*, vol. 78, pp. 388–399, Sep. 2019, doi: 10.1016/J.COMPELECENG.2019.08.004.
[27] P. Rajpurkar *et al.*, "Deep learning for chest radiograph diagnosis: A retrospective comparison of the CheXNeXt algorithm to practicing radiologists," *PLOS Medicine*, vol. 15, no. 11, p. e1002686, Nov. 2018, doi: 10.1371/JOURNAL.PMED.1002686.
[28] T. K. K. Ho and J. Gwak, "Multiple Feature Integration for Classification of Thoracic Disease in Chest Radiography," *Applied Sciences 2019, Vol. 9, Page 4130*, vol. 9, no. 19, p. 4130, Oct. 2019, doi: 10.3390/APP9194130.
[29] E. Ayan and H. M. Ünver, "Diagnosis of pneumonia from chest X-ray images using deep learning," *2019 Scientific Meeting on Electrical-Electronics and Biomedical Engineering and Computer Science, EBBT 2019*, Apr. 2019, doi: 10.1109/EBBT.2019.8741582.
[30] T. Rahman *et al.*, "Transfer Learning with Deep Convolutional Neural Network (CNN) for Pneumonia Detection Using Chest X-ray," *Applied Sciences 2020, Vol. 10, Page 3233*, vol. 10, no. 9, p. 3233, May 2020, doi: 10.3390/APP10093233.
[31] A. K. Jaiswal, P. Tiwari, S. Kumar, D. Gupta, A. Khanna, and J. J. P. C. Rodrigues, "Identifying pneumonia in chest X-rays: A deep learning approach," *Measurement*, vol. 145, pp. 511–518, Oct. 2019, doi: 10.1016/J.MEASUREMENT.2019.05.076.
[32] V. Chouhan *et al.*, "A Novel Transfer Learning Based Approach for Pneumonia Detection in Chest X-ray Images," *Applied Sciences 2020, Vol. 10, Page 559*, vol. 10, no. 2, p. 559, Jan. 2020, doi: 10.3390/APP10020559.
[33] R. Karthik, R. Menaka, and M. Hariharan, "Learning distinctive filters for COVID-19 detection from chest X-ray using shuffled residual CNN," *Applied Soft Computing*, vol. 99, p. 106744, Feb. 2021, doi: 10.1016/J.ASOC.2020.106744.
[34] E. E.-D. Hemdan, M. A. Shouman, and M. E. Karar, "COVIDX-Net: A Framework of Deep Learning Classifiers to Diagnose COVID-19 in X-Ray Images," Mar. 2020, Accessed: Feb. 08, 2022. [Online]. Available: https://arxiv.org/abs/2003.11055v1
[35] B. Antin, J. Kravitz, and E. Martayan, "Detecting Pneumonia in Chest X-Rays with Supervised Learning."
[36] P. K. Sethy and S. K. Behera, "Detection of Coronavirus Disease (COVID-19) Based on Deep Features," Mar. 2020, doi: 10.20944/PREPRINTS202003.0300.V1.
[37] K. Zrar *et al.*, "Diagnosing COVID-19 pneumonia from x-ray and CT images using deep learning and transfer learning algorithms," *https://doi.org/10.1117/12.2588672*, vol. 11734, no. 12, pp. 99–110, Apr. 2021, doi: 10.1117/12.2588672.
[38] R. Kundu, P. K. Singh, M. Ferrara, A. Ahmadian, and R. Sarkar, "ET-NET: an ensemble of transfer learning models for prediction of COVID-19 infection through chest CT-scan images," *Multimedia Tools and Applications*, vol. 81, no. 1, pp. 31–50, Jan. 2022, doi: 10.1007/S11042-021-11319-8/TABLES/9.
[39] E. H. Houssein, Z. Abohashima, M. Elhoseny, and W. M. Mohamed, "Hybrid quantum-classical convolutional neural network model for COVID-19 prediction using chest X-ray images," *Journal of Computational Design and Engineering*, vol. 9, no. 2, pp. 343–363, Apr. 2022, doi: 10.1093/JCDE/QWAC003.
[40] U. Sait *et al.*, "Curated Dataset for COVID-19 Posterior-Anterior Chest Radiography Images (X-Rays).," vol. 3, 2021, doi: 10.17632/9XKHGTS2S6.3.
[41] "NIH Chest X-ray dataset | Cloud Healthcare API | Google Cloud." https://cloud.google.com/healthcare-api/docs/resources/public-datasets/nih-chest (accessed May 30, 2022).
[42] "TBX 11 | Kaggle." https://www.kaggle.com/datasets/usmanshams/tbx-11 (accessed May 30, 2022).
[43] "EfficientNet: Rethinking Model Scaling for Convolutional Neural Networks." http://proceedings.mlr.press/v97/tan19a.html (accessed May 30, 2022).
[44] "EfficientNetV2: Smaller Models and Faster Training." http://proceedings.mlr.press/v139/tan21a.html (accessed May 30, 2022).
[45] "Transfer learning and fine-tuning | TensorFlow Core." https://www.tensorflow.org/guide/keras/transfer_learning (accessed May 30, 2022).
[46] "Lookahead Optimizer: k steps forward, 1 step back." https://proceedings.neurips.cc/paper/2019/hash/90fd4f88f588ae64038134f1eeaa023f-Abstract.html (accessed May 30, 2022).
[47] L. Liu *et al.*, "On the Variance of the Adaptive Learning Rate and Beyond," Aug. 2019, doi: 10.48550/arxiv.1908.03265.